

# Seismic Analysis of RC Flat Bottom Circular Clinker Silos

T. Sharaf<sup>1\*</sup>, M. Hassan<sup>2</sup> & O. M. Ramadan<sup>3</sup>

<sup>1</sup> Faculty of Engineering, Port Said University, Port Said, Egypt.

<sup>2</sup> Faculty of Engineering, Cairo University, Cairo, Egypt.

<sup>3</sup> Faculty of Engineering, Cairo University, Cairo, Egypt.

\* Corresponding Author: tarek.sharaf@eng.psu.edu.eg

**ABSTRACT:** This research addresses the nonlinear analysis of flat bottom clinker silos that are typically used to store granular materials. Most of silos' failure is due to the inefficiency to resist seismic forces. One of the silo failure reasons is that filled granular material is usually treated as a water pressure which is not realistic. Water pressure is linearly distributed, while granular material has a nonlinear distribution along silo height. The main investigated variables were silo width, height, reinforcement ratio, and the existence of opening in the bottom part of the silo wall. Effects of these variables on silos' dynamic properties - modal periods and mode shapes - as well as seismic response, base shear, base overturning moment, and the least number of modes needed to satisfy mass participation of 90%, were examined. Extensive numerical analyses were conducted to examine these parameters using different types of analyses such as free vibration, response spectrum, and pushover analysis. It was found that increasing height has a great effect on time-period when compared to the effect of diameter increase. Reinforcement ratio in silo without openings has a minor effect in small diameters while it has a major effect in case of silos with large diameters.

**Keywords:** Seismic Analysis; Pushover Analysis; Free Vibration; Response Spectrum; Buckling Mode; Clinker Silos.

## 1 INTRODUCTION

Silos are very common structures which are used in industrial and agriculture sectors. Despite the technological development in the silo's construction field but there's a lack in estimating the nonlinear behavior of granular material inside the silo. To understand all these critical aspects, the researchers devoted their efforts to study these issues like estimating the nonlinear behavior of granular material during earthquake actions and its effect on the silo wall pressures and stresses as well as the effect of filling and discharging on the silo's behavior during seismic loads.

Some silos' reported failures were due to carbonation of concrete, reinforcement corrosion, loss of concrete cover, changes in silos utilization and excessive deformation due to loss of ability to resist lateral loads, Maj (2017). ACI (1996) includes the design of silos and stacking tubes to store granular materials with no special classifications for contained materials. On the other hand, EUROCODE (2006) divides silos according to actions and design purpose. ACI calculates static pressure inside silos considering the at rest load case, while EUROCODE

(2006) divided loads according to the type of the stored material and provided methods to calculate solid parameters using experimental tests. Carson and Craig (2015) studied the inconsistencies between the most current common codes. The study showed that the most reasons that led to failure that designers simulated granular material as a fluid which is not true as in the fluid case the maximum pressure on the wall occurred at the bottom portion of the wall, while for granular materials, the pressure is maximum in the middle. Abbas (2014) studied numerically the free vibration characteristics and seismic response for elevated flat bottom clinker silos supported on wall. A comparison with applying silo initial load distribution is calculated using Janssen's method (1895).

Castiglioni and Kanyilmaz (2015) found that most of the existing silos were not designed for the new design code recommendation to resist earthquake loads. Abdel-Rahim (2014) studied seven reinforced concrete silos using different heights to diameters ratio with and without earthquake loads considering filling and discharging pressure. The study showed that squat silos with  $h/d = 1$  to 2 had more resistance to earthquake and were more economical. Also, vertical earthquake loads had a small effect on heavy silo structures while lateral loads had more effect on

taller silo structures.

Togarsi (2015) studied the effect of nonlinear seismic behavior of reinforced concrete silos by comparing the results of displacement and vibration analysis of two concrete silos supported on columns and the other supported on shear walls and columns respectively. The study was considered empty, partially filled, and full of granular material. It was found that models with columns only has the largest top displacement, and the case of full silo had the largest displacement. Jagtap et al. (2014) studied the nonlinear behavior of granular material cylindrical steel silo exposed to dynamic base excitation using three-dimensional finite element modelling. On the other hand, Niemunis and Herle (1997) and von Wolffersdorff (1996) took the effect of intergranular strain in the hypoplastic constitutive model into consideration. The aim was to develop a comprehensive three-dimensional granular material silo that includes all possible sources of nonlinearity for static and dynamic analysis.

Jagtap et al. (2014) compared between static finite element analysis and Janssen's theory (1895). It was shown that the two methods agreed with a small difference depending on the linear-elastic constitutive behavior of the granular material. Results of ground motion were compared using Eurocode8 part4 [14], and it was found that Eurocode is conservative. Pieraccini et al. (2017) presented an analytical formulation based on the Pieraccini (2015) and Silvestri (2012) theory to determine the natural frequency for grain silo. The silo was simulated as an equivalent shear-flexural cantilever beam with an applied mass equal to the silo structure plus the mass of the portion of the stored material. It was found that grain silos have strong nonlinear dynamic behavior, also the silos are affected by the dynamic input and the stored material properties. There is a difficulty in the prediction of the behavior of grain silos under seismic excitation. Butenweg (2017) presented a comparison between static equivalent loads acting on the cylindrical silo and the time history analysis considering the nonlinearities induce by the filling processes and the interaction between silo wall and the stored granular material. The behavior of granular material using hypoplastic material model was based on the formulation of Gudehus (1996). The model was validated by the shaking table tests carried out by Holler and Meskouris (2006). Nateghi and Yakhchalian (2011) and Beg, Yadav (2017) [22]. Beg, Yadav (2017) found that pressures inside silos are affected by silo type, silo wall type, stored material properties, the mass flow pattern, and eccentric flow. As for the discharge rate, El-Arab (2014) studied flow patterns and wall pressures induced during the filling and emptying processes of silos, experimentally and numerically. It was found that design

codes depend on Janssen's method (1895) to calculate the pressures on the silo wall, and it is only applicable for bins which have symmetrical cross-sections, and the material case is in at rest load case. Also, the measured pressure due to non-symmetric dynamic discharge did not agree with that of the design codes which gave overpressure factors to overcome this problem. The study general outcomes agreed with the outputs of Rombach and Neumann (2004). Gallego et al. (2015) compared experimental and finite element results of cylindrical silo filled with wheat grains by measuring the normal pressures and friction forces in the silo wall during filling and discharging cases. The study showed that mass flow inside the silo is better than the funnel flow and this can be achieved by smooth hopper wall with large outlets.

The current research aims to study the effect of stored granular material inside the silo, openings size, height change, silo diameter, and reinforcement ratio, on the behavior of silo during earthquake. Also, proposing simplified equations to predict the fundamental period of such silos in relation with opening size and height.

## 2 STRUCTURAL MODELLING

In this present study the numerical model for finite element simulated using ANSYS (2016). A total of 240 models were accomplished for heights-to-diameter ratios of 1.5, 2.0, 2.5, and 3.0, and with diameters of 7 m, 10 m, 15 m, 18 m, and 20 m. Effect of openings on seismic behavior has been observed by simulating two access opening 3.5 m \* 4 m, as shown in Figure (1).

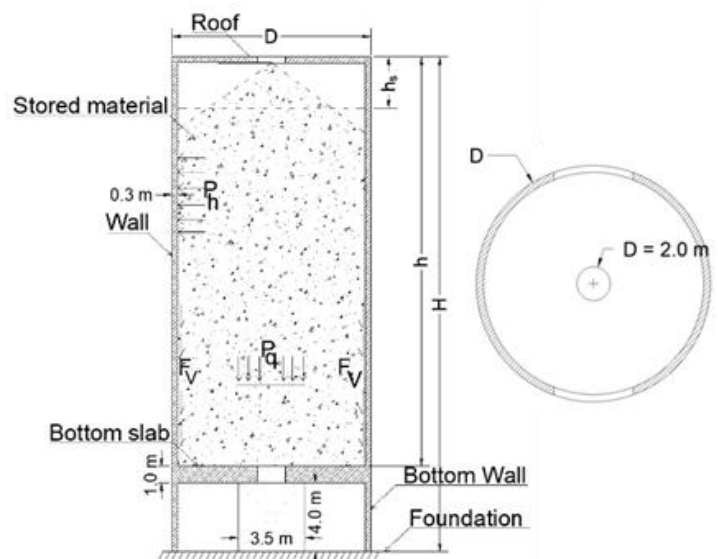


Figure 1. Silo typical model showing openings locations (dimensions are in m).

The numerical model for the finite element simulation consists of three components, namely the silo concrete elements, the granular material, and the interface between the silo walls and the granular material. The silo wall is modeled by solid element 65 as it has capabilities of cracking in tension and crushing in compression. The concrete is capable of cracking (in three orthogonal directions), crushing, plastic deformation, and creeping. Figure (2a) shows the eight nodes solid 65 geometry with the capability of having three rebars in three different dimensions. The silo wall and the reinforcement are simulated using 5 layers through the wall thickness. Two layers of reinforcements, with smeared reinforcement model, were used to model the top and bottom reinforcements inside the silo wall with thickness of 50 mm, as shown in Figure (2b). The other three layers were used to model the outer and inner concrete cover from one side and the concrete core from the other side.

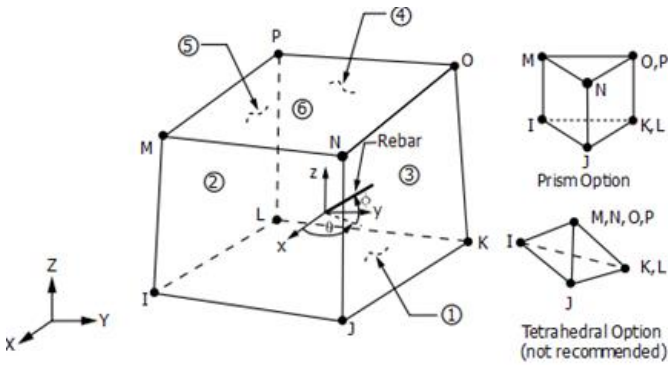


Figure 2a. Finite element Solid 65, ANSYS.

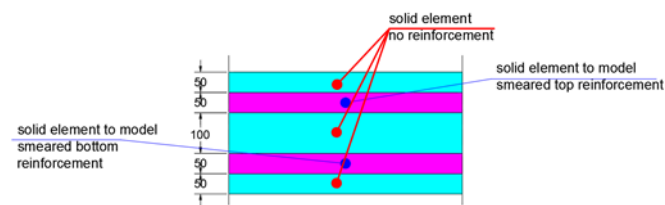


Figure 2b. silo wall thickness element divisions.

Free vibration analysis and response spectrum analysis has been performed through a linear model of concrete material. Consequently, the properties of linear concrete material are shown in Table (1) according to EUROCODE (2006). Material properties of the filling material are obtained from Arar (2016) as young's modulus of grains is 136100 MPa with 2.05 t/m<sup>3</sup> density, Poisson's ratio is 0.36 and the coefficient of friction against silo's wall is 0.05. The geometric compatibility between the granular material silos contents and the silo walls is enforced by means of special three-dimensional nonlinear surface to surface contact element (CONTA-174& TARGE170). These bipartite contact elements have one side attached to the surface of the granular mate-

rial (CONTA-174) and an associated target element attached to the inside of the silo wall (TARGE170).

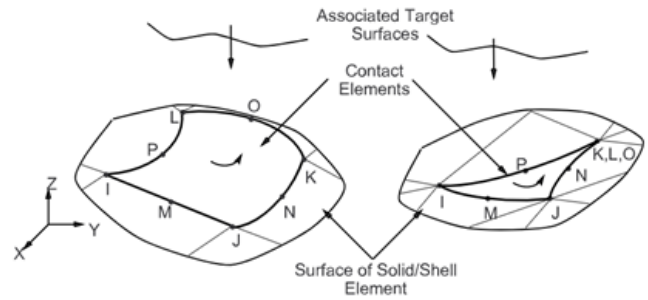


Figure 3. ANSYS contact pairs, CONTA174 and TARGE170

Table 1. linear properties of concrete, Grain properties.

Linear properties of concrete	
fck (cylinder strength)	32 MPa
fcu (cubic strength)	40 MPa
Poisson's ratio	0.2
Ec (Young's modulus)	33345 MPa
γc (weight per 1 m <sup>3</sup> volume)	2.5 t/m <sup>3</sup>

The regarded flat bottom silo has a constant top slab thickness of 300 mm. An inner circular opening has a constant diameter of 2.0 m. The bottom slab has a constant thickness of 1000 mm. Figure (4) shows the three-dimensional (3D) silo model with a fixed boundary condition at the base. In addition, the figure shows the top and bottom slab with 2000 mm opening size as well as the silo circular wall. The silo top wall is a solid with a constant thickness of 300 mms for all models used in this research. Due to the stored material, this wall is exposed to horizontal pressure as well as vertical friction. The bottom silo wall was modelled with a 300 mms constant thickness with 4.0 m height. In the case of silo wall with openings in the bottom wall, the access openings are 3.5 m width and 4.0 m height.

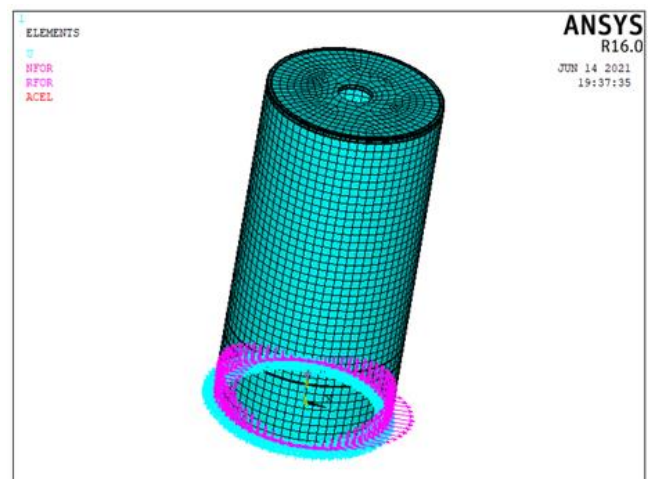


Figure 4. Three-dimensional FE silo model.

### 2.1 Mesh sensitivity analysis

Two different analyses were implemented in order to perform a mesh sensitivity analysis, the first analysis was static analysis while the latter was a response spectrum analysis. Static analysis was implemented using two types of loads, 1000 kN concentrated load at the silo top edge, and the second load was distributed load of 100 kN/m along the silo height, as shown in Figure (5). Mesh sensitivity analysis was carried out on one model with 15.0 m diameter and height-to-diameter ratio of 1.5. The analysis considered two cases of the silo, empty and full of grains.

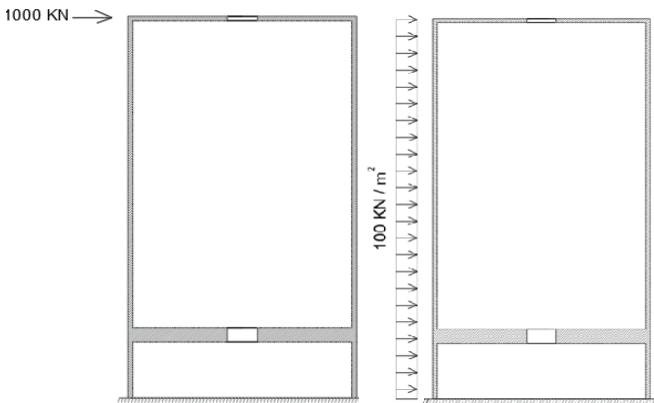


Figure 5. Lateral load type: Concentrated load (left) and distributed load (right).

#### 2.1.1 Static analysis

Figure (6a), and Figure (6b) show the maximum displacement for full and empty silo, respectively, so due to stiffness of the bottom slab the curve have a significant change at height 5m, also due to top slab and location of the load the displuming increased. Four mesh sizes have been examined, 0.25 m, 0.5 m, 0.75 m, and 1 m. For the 1000 kN concentrated top load, the results show that there was almost no difference between the four mesh sizes results used to model the silo. So, 0.5 m mesh size was chosen for all silo models to minimize the run time and at the same time to obtain a smoother deformed shape.

Figure (7a), and Figure (7b) show the maximum displacement for full and empty silos, respectively, for the 100 kN/m distributed load. In case of full silo, the curve has a linear distribution due to the fixed stiffness of the grains along the height of the silo. Again, there was no noticeable difference among the tested mesh sizes, so the mesh size of 0.5 m was the most appropriate mesh size to be used for silo models herein in this research.

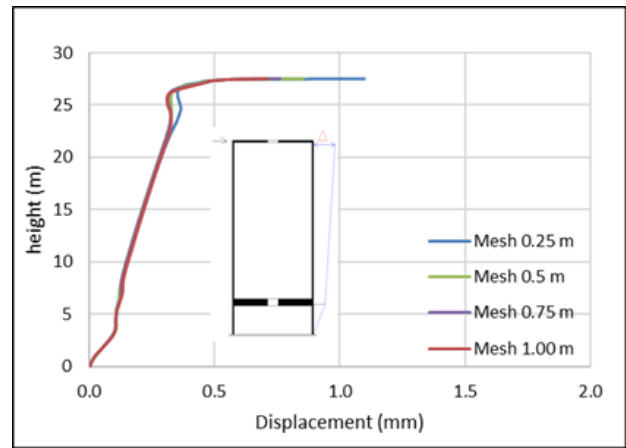


Figure 6a. Silo lateral displacement under concentrated load (D= 15.0 m and H/D =1.5) for Full silo.

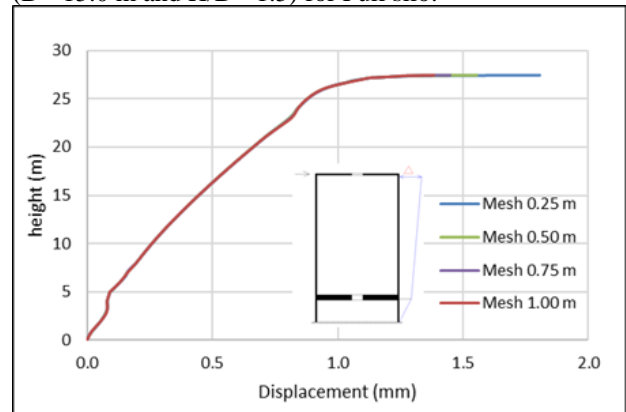


Figure 6b. Silo lateral displacement under concentrated load (D= 15.0 m and H/D =1.5) for Empty silo.

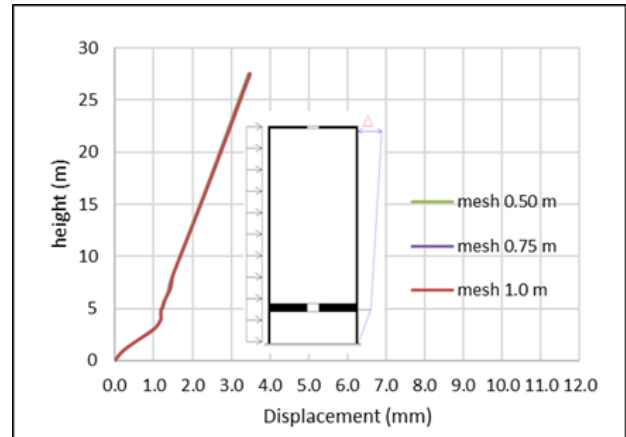


Figure 7a. Silo lateral displacement under distributed load (D= 15.0 m, H/D = 1.5) for full silo.

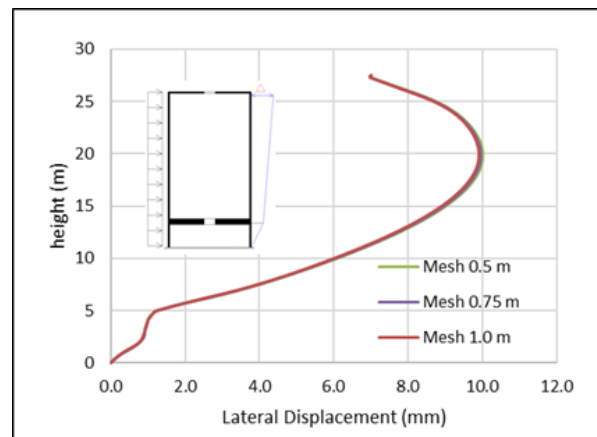


Figure 7b. Silo lateral displacement under distributed load (D= 15.0 m, H/D = 1.5).

### 2.1.2 Response spectrum analysis

Dynamic analysis has been performed using response spectrum analysis according to EUROCODE8 (2005). Seismic analysis was implemented using Type 2 of seismic with deposits of loose-to-medium cohesionless soil which is classified as soil class D.  $\gamma_I$  is the importance factor, and Eurocode recommends a value of 1.2 for buildings such as silos. The silos in the current research had been considered laying in a zone for which the acceleration gravity  $a_g = 0.15 g$ , which  $g$  is the gravitational acceleration,  $9.81 \text{ m/s}^2$ . The following factors are derived from the Eurocode:  $T_B = 0.1$ ,  $T_C = 0.3$ ,  $T_D = 1.2$ , and  $S = 1.8$ . Figure (8) shows the response spectrum Type 2 curve. Three mesh sizes were checked, namely, 0.5 m, 0.75 m, and 1 m. Figure (9a), and Figure (9b) show the average displacement for full and empty silo, respectively, and the figure shows that the results are almost identical, due to the mass of the grains the displacement increased in case of full silo than the empty.

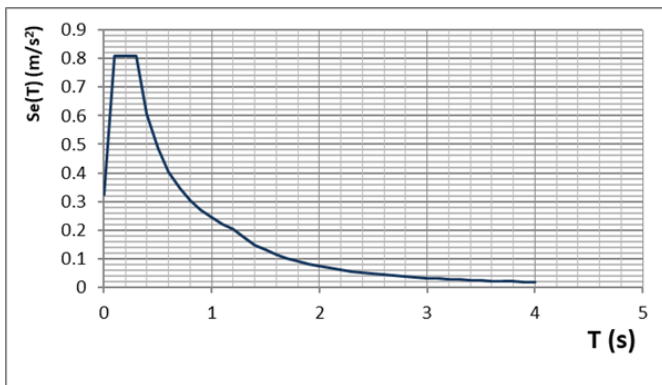


Figure 8. Response spectrum type 2 curve, EUROCODE8 (2005).

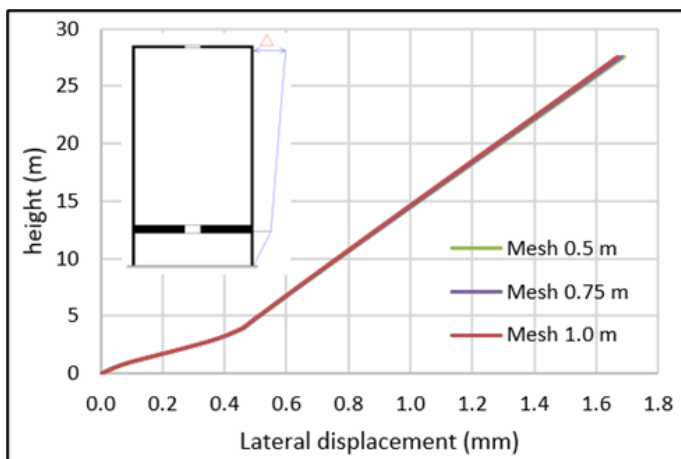


Figure 9a: Full silo lateral displacement for various mesh sizes ( $D = 15.0 \text{ m}$  and  $H/D = 1.5$ ).

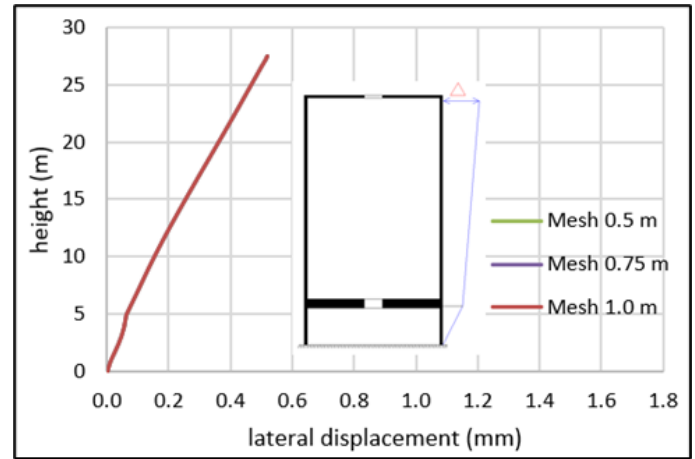


Figure 9b: Empty silo lateral displacement for various mesh sizes ( $D = 15.0 \text{ m}$  and  $H/D = 1.5$ ).

Mesh size of 0.25 m was a very time-consuming size, and it gives results almost identical to the results of mesh size 0.5 m. So, a Mesh size of 0.5 m was used for all models within the current study.

## 3 FREE VIBRATION ANALYSIS

A free vibration analysis was implemented in order to monitor the differences in silo behavior with various parameters such as silo height, silo diameter, silo bottom wall openings, and different reinforcement ratios. Used reinforcement ratios ( $\mu$ ) were 1 %, 0.6 %, and 0.2 % of the total concrete cross sectional area, the same ratios were used typically for vertical and horizontal reinforcements.

### 3.1 Effect of height and diameter

A total of 240 FE models were simulated in order to study the effect of height and diameter on the fundamental period. The results showed that the fundamental period increases with increasing the height and the diameter showing that mass had more impact than stiffness on the fundamental period. It was noticed that increasing the reinforcement ratio led to an increase in the fundamental period due to increasing the ductility of the structure. In the case of silo diameter of 10 m without openings and with height-to-diameter ratio of 1.5 and  $\mu = 0.6\%$ , the fundamental period ( $T$ ) was 0.155 sec. While for silo diameter of 10 m,  $\mu = 0.6\%$  and a height-to-diameter ratio of 2.0,  $T = 0.212$  sec. The fundamental period was 0.277 sec in the case of height-to-diameter ratio 2.5 and it was 0.35 sec for height-to-diameter ratio of 3.0. So, the increasing silo height led to an increase in the time period as the stiffness decreased. For silo diameter 15 m, without openings, and with height-to-diameter ratio of 1.5 and  $\mu = 1\%$ ,  $T = 0.216$  sec which was less than 0.297 sec for same si-

lo diameter and reinforcement ratio but with height-to-diameter ratio of 2.0.  $T = 0.39$  sec for the same silo with height-to-diameter ratio of 2.5, and  $T = 0.495$  sec for height-to-diameter ratio of 3.0. It was noticed that full of grains silo gave more fundamental time period when compared to empty silo for all cases of openings. The differences occurred because grains weight led to an increase in the total mass which showed that mass had more significant effect than the stiffness.

Likewise, the effect of increasing silo height was more than the effect of increasing the diameter, as shown in Figure (10), for the full silo without openings with  $\mu = 1\%$  because of effect of the height in the total weight of the silo is more than effect of the diameter. Furthermore, the ratio between fundamental periods for different diameters is increasing with increasing silo height.

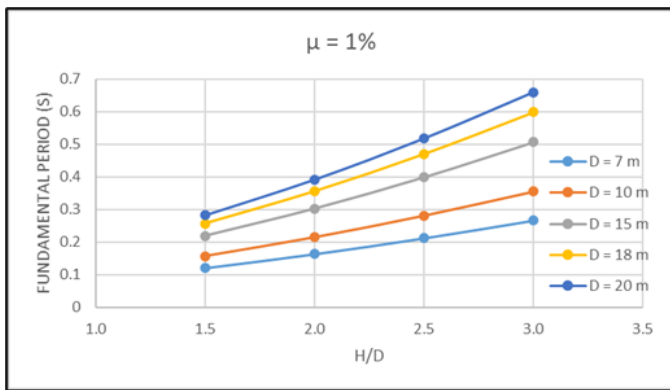


Figure 10. Fundamental period for full silo without openings for  $\mu = 1\%$ .

Figure (11a) and (11b) show the relation between fundamental period and silo height for full and empty silo, without opening, respectively. It can be seen that, increasing the silo diameter has a significant effect on the empty silo than the full silo. It is seen that empty silo with  $D = 20$  m, the fundamental period is constant for height  $\leq 45$  m while for less diameters, the fundamental period is increasing gradually. Because full silo is more critical than empty silo as it has a more fundamental period, the full silo results will be shown in the following sections.

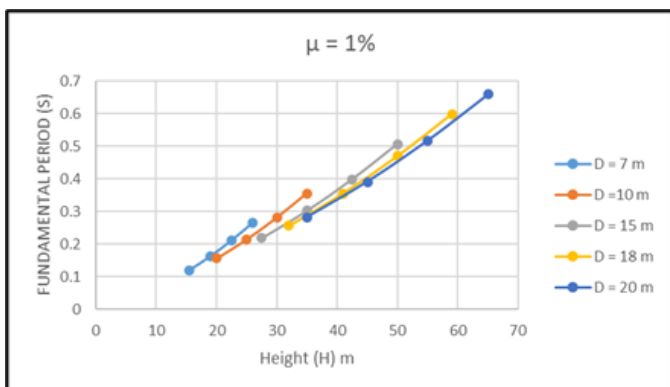


Figure 11a. Fundamental periods vs Height for full silos without opening ( $\mu = 1\%$ ).

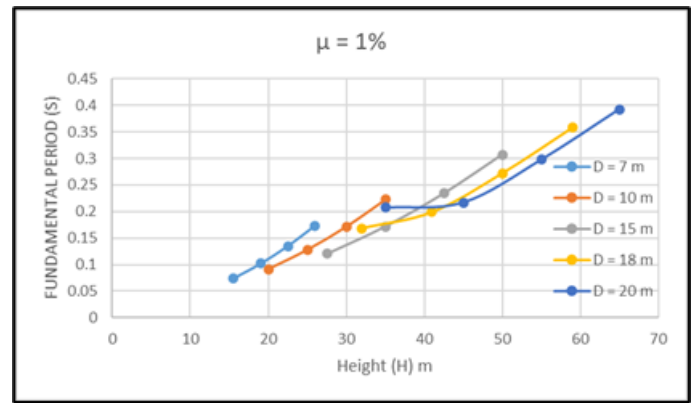


Figure 11b. Fundamental periods vs Height for empty silos without opening ( $\mu = 1\%$ ).

### 3.2 Effect of openings

It was found that the openings existence led to an increase in the fundamental period values due to the stiffness reduction, as shown in Figure (12). It is observed that the fundamental period for silos with opening is almost 14 % more than the solid empty one at  $H/D = 1.5$  and, while it is 16 % more for  $H/D = 3.0$ . For silos with openings, as the height to diameter ratio increases, the fundamental period increases. Also, by increasing silo's height and diameter, the silo's overall weight effect increases and leads to higher fundamental periods. Table (2) shows the ratios of fundamental periods of silos with and without openings. It is obtained that while the ratio of opening perimeter to the total perimeter ( $\lambda$ ) = 36 % the ratio of the fundamental periods was 45 % at diameter 7 m, and it continued to decrease for larger diameters at which the fundamental period ratio reached 9 % at  $\lambda = 13\%$  and  $D = 20$  m.s.

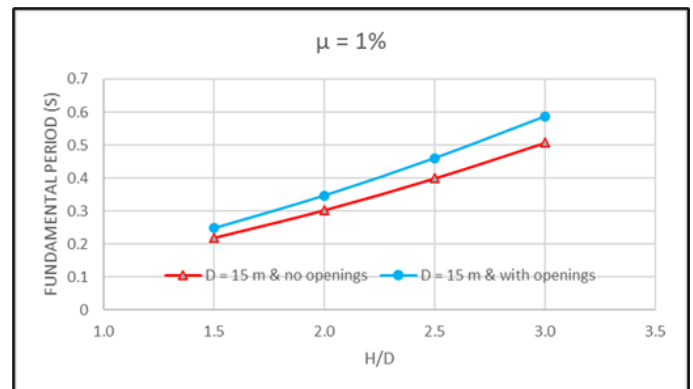


Figure 12. Fundamental period for full silo  $D = 15$  m with and without openings for  $\mu = 1\%$ .

Table 2. Ratio of fundamental periods for silos with  $\mu = 0.6\%$  (with opening and without opening for  $H/D = 1.5$ ).

Diameter	A= (T with opening/ T without)	$\lambda =$ (opening perimeter/ Total silo perimeter)
7 m	1.446247	0.36
10 m	1.24286	0.25
15 m	1.131457	0.17
18 m	1.102616	0.14
20 m	1.089205	0.13

Figure (13) shows three values of the fundamental period at silo height 35.0 m for silo diameter 10m, 15m, and 20m, since increasing the diameter leads to increase the stiffness so fundamental period decreases. In the case of the full silo with openings the values are 0.45557 sec, 0.34742 sec and 0.30760 sec for diameters 10m, 15m, 20m respectively for 1 % reinforcement that means the silo diameter 10m has less stiffness than the others since it the least diameter. In the case of the full silo with opening the values are 0.58690 sec and 0.52733 sec for diameters 15m and 18m respectively for 1 % reinforcement. From these results it is observed that at the same height the lower diameters have less stiffness, so they have more fundamental periods.

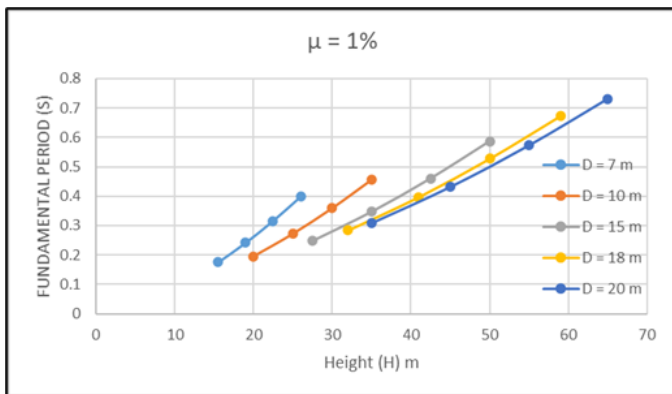


Figure 13. Fundamental periods vs height, full silo with openings ( $\mu = 1\%$ ).

### 3.3 Effect of reinforcement ratio on the fundamental period

Three reinforcement ratios 1 %, 0.6 % and 0.2 % were investigated for all cases of silos were studied herein. It is obtained from Figure 14 that the reinforcement ratio does not have a significant effect on the fundamental period of the silo, as the curves are almost identical. The effect of reinforcement in linear analysis depends on its weight and it is very minor compared with the concrete silo's weight.

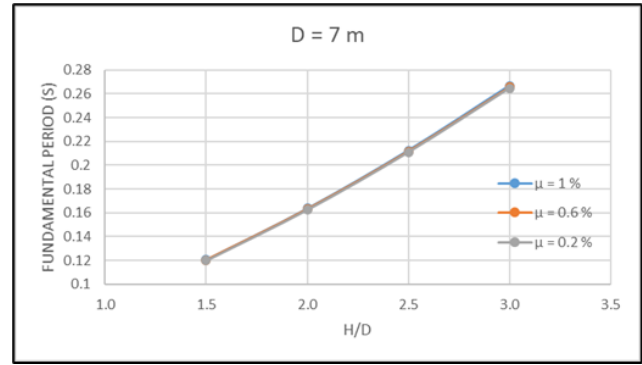


Figure 14: Fundamental period for full silo  $D = 7\text{ m}$  without opening for different reinforcement ratios and different height to diameter ratios.

### 3.4 Estimating the fundamental period

An analytical formula is needed to estimate the fundamental period for clinker silos for full silo in all its cases using curve fitting method to design the silos safely and rapidly. Curve fitting had been done for curves between fundamental period and height, as from previous sections in this research, it is obtained that increasing the height has more effect on fundamental period than increasing the diameter. As the reinforcement has no significant effect on the clinker silo fundamental period as proved earlier in this research,  $\mu = 0.6\%$  is to be used to investigate the formulas. Figure 15, and Figure 16 show the used curves to estimate the formulas for the fundamental period with height for silo different cases. It is obtained from the curves that in case of full silo without openings the equation is  $T = 0.0055H^{1.1372}$ , in case of full silo with openings  $T = 0.0142H^{0.9238}$ .

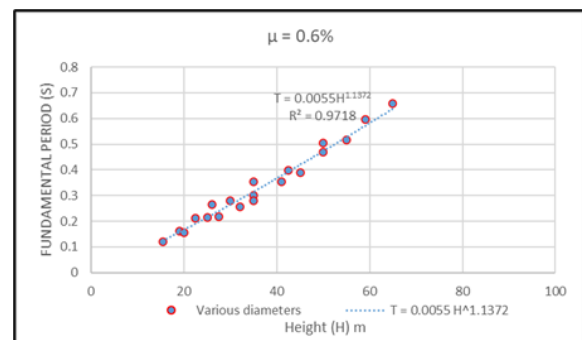


Figure 15. Fundamental period formulas ( $T \propto H$ ) for full silo without openings for various diameters for  $\mu = 0.6\%$ .

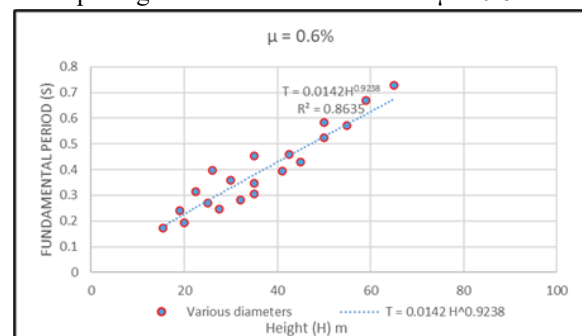


Figure 16: Fundamental period formulas ( $T \propto H$ ) for full silo with openings for various diameters for  $\mu = 0.6\%$ .

### 3.5 Model shapes

The first 12 modes had been chosen to be presented with mass participation factors in this part for four types of silos for 15 m silo diameter and height to diameter ratio is 1.5. The first mode shape was the dominant one in all models and its type is lateral mode shape. Figure 17, and Figure 18 show the mass participation factor for the first 12 modes for empty and full silo without openings. It is obtained that for full silo without openings shows that mode (1) has a mass equal 0.86086 with lateral mass type in X-direction, mode (2) in Y-direction and mode (3) is torsion as appearing in Figure 19. The summation of mass has more than 90 % at mode (6) for X-direction and mode (5) for Y-direction as recommended from ASCE-SEI05 [17] that mass participation factor must be more than 90 %. The rest of mode shapes do not have a significant effect, as it has a small mass. In the case of the empty silo without openings summation of mass reached 90 % at mode (18) for X-direction and mode (19) for Y-direction. Likewise, in the case of full of grains silo with openings summation of mass has more than 90 % at mode (2) for X-direction and mode (6) for Y-direction. Furthermore, in the case of the empty silo with openings Summation of mass reached 90 % at mode (14) for X-direction and mode (19) for Y-direction. It is obtained from these results that full silo has a behaviour near to cantilever as it is collecting the 90 % masses in early mode shapes, on the contract the empty silo collects the 90 % mass participation factor after more numbers of mode shapes.

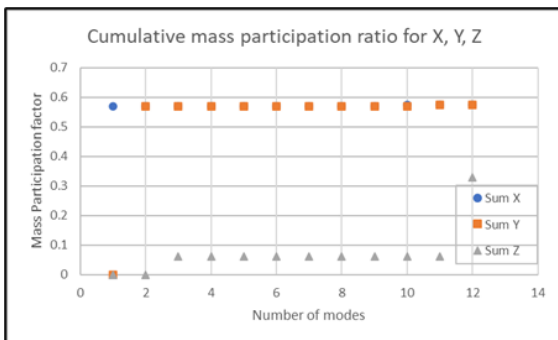


Figure 17: Mass participation ratios for first 12 modes empty silo without openings for D = 15m and H/D = 1.5.

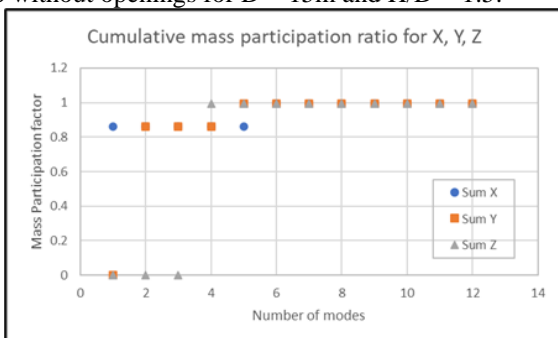


Figure 18: Mass participation ratios for first 12 modes full silo without openings for D = 15m and H/D = 1.5.

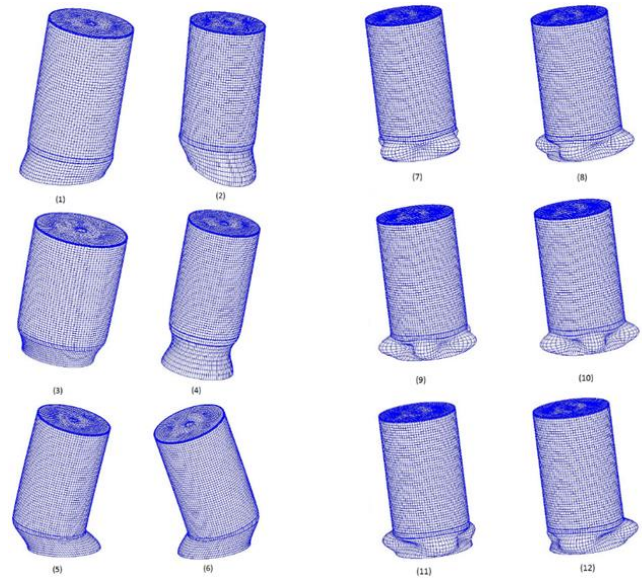


Figure 19: The first 12 mode shapes of full silo without openings D = 15 m and H/D = 1.5

## 4 RESPONSE SPECTRUM ANALYSIS

Response spectrum analysis (RSA) is a method to estimate the structural response due to a combination of earthquakes that may probably happen in the same region. RSA is an elastic-linear dynamic analysis which is a superposition of mode shape results by summation results for the number of modes which has a 90 % mass participation factor as mentioned earlier. RSA was carried out for all presented silos in this study in two orthogonal directions X and Y directions. ANSYS [14] had been used to do this analysis and show the maximum base shear, displacement, and overturning moment due to response spectrum analysis.

### 4.1 Number of modes

Free vibration analysis was developed to detect the number of modes which has a mass participation factor of more than 90%. Twelve modes had been chosen to be the minimum number of modes to be considered. Figure 20 shows the relationship between the number of modes and H/D for full silos with and without openings for X and Y directions for 1 % reinforcement ratio respectively. It is obtained that in all full of grains silo cases in X and Y directions with and without openings number of modes are 5 modes for  $H/D \geq 2.5$ , 6 modes in case of  $H/D \leq 2.0$ , as it works as a cantilever near to first mode shape. on the contrary in empty silo cases number of modes varies from 3 in the case of the empty silo with openings with D = 7.0 m and H/D = 2.0 to 55 in the case of the empty silo with openings with D = 20 and H/D = 3.0, as it vibrates freely since,

it has not a big mass like full silos. The curves show also that there is a non-significant difference between the number of modes in the X and Y direction in the case of silos without openings. On the other hand, in the case of opening existence, there is a significant change in the number of modes between the X and Y direction, as the openings have an effect in the stiffness in one direction more than the other. The number of modes for full of grains silo with openings with  $D = 7.0$  m and  $H/D = 1.5$  in the X direction is 2 modes, but in Y direction is 6 modes. Likewise, the number of modes varies between 3 and 16 for empty silos with openings in X and Y directions respectively. It is obtained also that the reinforcement ratio does not have any effect on the number of extracted modes to perform response spectrum analysis.

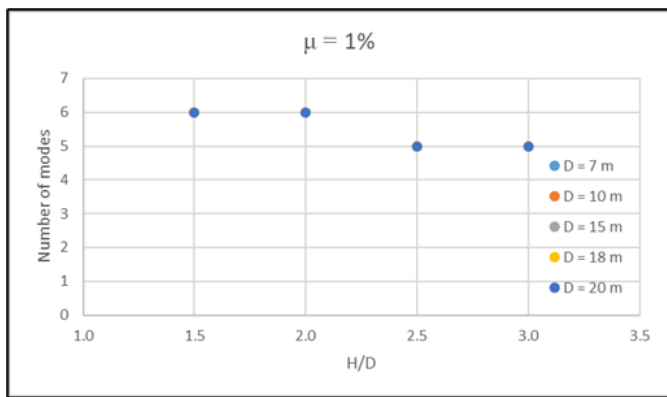


Figure 20: Number of modes for mass distribution factor more than 90 % for full silos without openings in X direction.

#### 4.2 Response spectrum analysis results

From the results, it has been observed that with increasing the diameter and the height, the base shear increasing due to mass increasing. For instance, full of grains silo diameter 7m, height to diameter ratio 1.5 without openings and reinforcement ratio 1 % the base shear is 706 KN. On the other hand, for full grains silo diameter 10 m, height to diameter ratio 1.5 without openings and reinforcement ratio 1 % the base shear is 1972 KN. So, the effect of diameter and height leads to increase the weight, so the correspondence base shear increases. Due to symmetry the base shear in X-direction and Y-direction are in agreement, but in the case of silos with openings base shear in X-direction is more than base shear in Y-direction as shown in Figure 21, and Figure 22 for full and empty silo with opening respectively for  $D=7.0$  m with various height to diameter ratio. In addition, the figures show the relation between the seismic coefficient ( $V$ =base shear/seismic weight) and  $H/D$ , it is obtained that the seismic coefficient decreases with increasing  $H/D$ , so the silos are more critical with decreasing  $H/D$ . It is obtained from the curves that the existence of openings leads to having

a difference in corresponding stiffness to be bigger in X-direction than Y direction as shown in the curves. Figures 23, and 24 show the relation between base shear and  $H/D$  for various height to diameter ratios for 1 % reinforcement ratio for full and empty silo. It is obtained from the curve that increasing the height and diameter leads to an increase in the base shear as the weights are increased. But in case of  $D-15, 18,$  and  $20$  m, the base shear is not incrementally increased and that is due to the higher mode has an effect in the silo behavior as shown in Figure 25, and 26 which show the mass participation ratio for full and empty silos.

The results show that with increasing the reinforcement ratio the base shear increases as shown in Figure 27 due to increasing the ductility and weight of reinforcement. Also, the results show that in the case of full silo without openings the reinforcement ratio has a minor effect in the case of silos with diameters 7, 10 m, but it has a major effect in the case of silo diameters 15 m, 18 m, 20 m in X and Y direction as the silos are taller and the mass of reinforcement increases. Likewise, in the case of empty silos, the reinforcement ratio has a major effect on base shear results for all silo diameters in the X and Y direction as shown in Figure 28 as the ratio of reinforcement weight to empty silo is bigger than case of full of grains silo. The same previous conclusions appear in the silo with an opening for full of grains and empty silos. Figure 29 shows the relation between height to diameter ratio with the overturning moment “ $M_y$ ” for full of grains silos and the results show that with increasing the silo height the overturning moment increases.

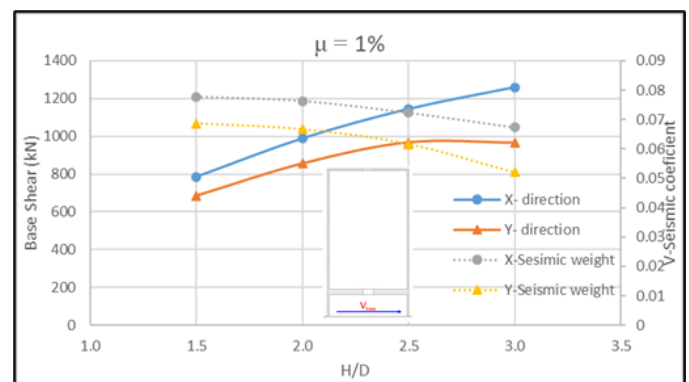


Figure 21: Base shear results for full silo with  $D = 7.0$  m with opening for various height-to-diameter ratios.

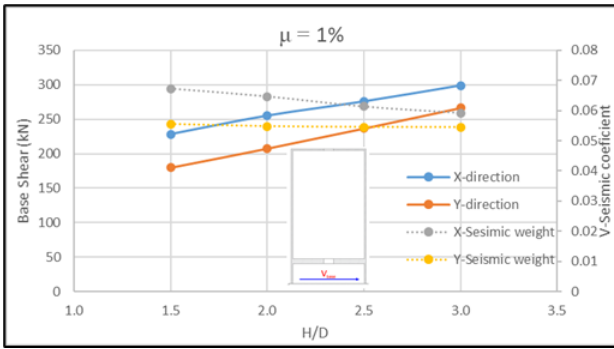


Figure 22: Base shear results for empty silo with  $D = 7.0$  m with opening for various height-to-diameter ratios.

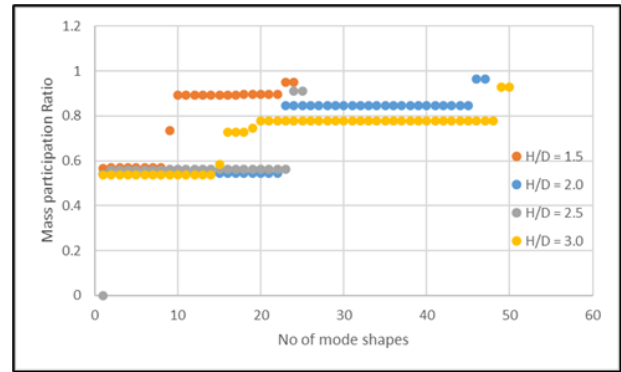


Figure 26: Mass participation ratios for empty silo without openings for  $D = 18$  m for various  $H/D$ .

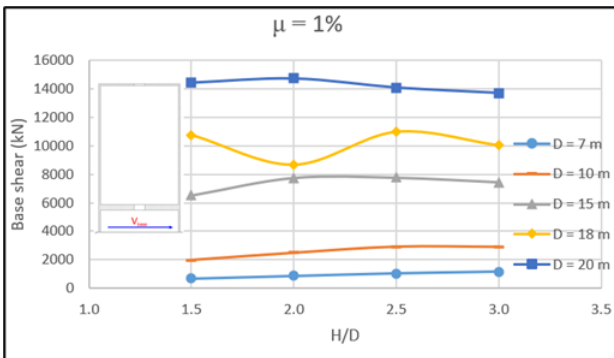


Figure 23: relation between Base shear and  $H/D$  for full silo for various height-to-diameter ratios with  $\mu = 1\%$ .

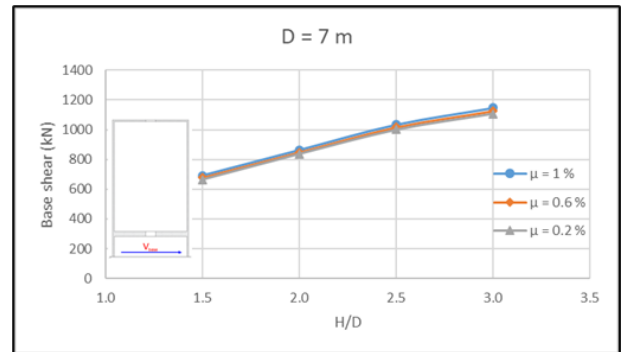


Figure 27: Base shear results for full silo with  $D = 7.0$  m for various height-to-diameter ratios with various reinforcement ratios.

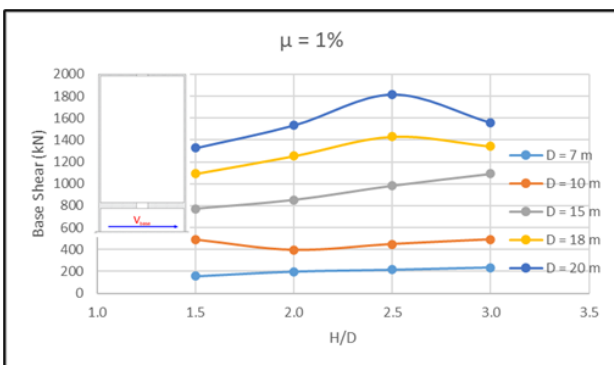


Figure 24: relation between Base shear and  $H/D$  for empty silo for various height to diameter ratio with  $\mu = 1\%$ .

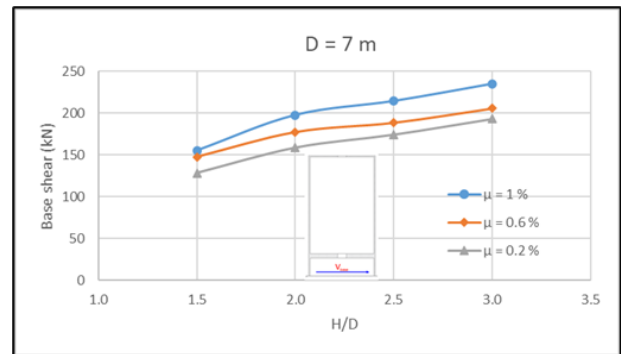


Figure 28: Base shear results for empty silo with  $D = 7.0$  m for various height-to-diameter ratios with various reinforcement ratios.

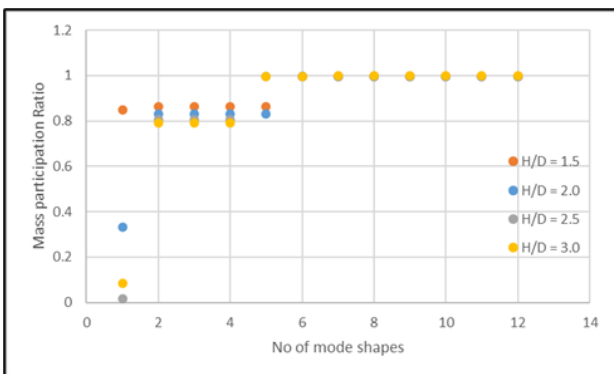


Figure 25: Mass participation ratios for full silo without openings for  $D = 18$  m for various  $H/D$ .

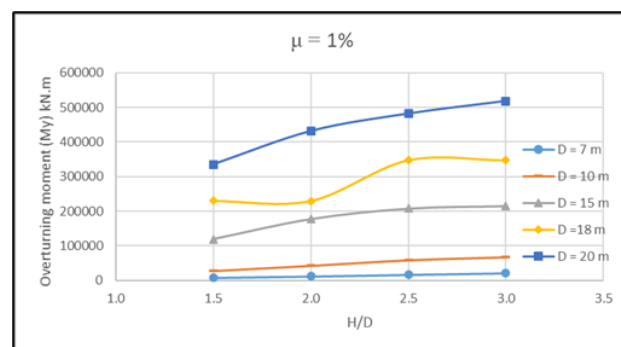


Figure 29: The relation between  $H/D$  and overturning moment  $M_y$  for full silos for  $\mu = 1\%$ .

5 PUSH-OVER ANALYSIS (NONLINEAR STATIC ANALYSIS)

5.1 Finite element modeling

A cylinder with 3 m diameter and 6 m height is used to establish the mesh sensitivity analysis. Due to the inappropriate results of the Smearred reinforcements method in nonlinear analysis, discrete reinforcement (REINF264) is used to model reinforcements inside the silo walls cross sections. Reference to Fanning 2001[18], the author concluded that the optimum modeling technique is Discrete reinforcement as it is better in controlling mesh density and gives more appropriate results than the Smearred one, so Discrete reinforcement is use herein. REINF264 is used to provide extra reinforcing to elements such as solid elements. The element is suitable for simulating reinforcing fibers with arbitrary orientations. Each link is used to model separately as a spar with only uniaxial stiffness. REINF264 has plasticity, stress stiffening, creep, large deflection, and large strain capabilities. Figure 30 shows REINF264 geometry and coordinate system.

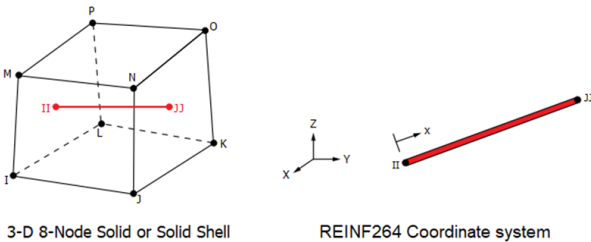


Figure 30: REINF264 geometry and coordinate system.

The stress strain curve suggested by Hognestad is used to model the concrete behavior as a mathematical model of the stress strain relationship of concrete under axial loading. The model suggested by Hognestad assumes the ascending branch and the descending branch as a second-order parabola and an oblique straight-line Figure 31a. Table 3 shows the properties of concrete applied in Ansys16 [14]. Reinforcement is modeled by bilinear model with  $f_y = 360$  MPa and young's modulus 210 GPa as shown in Figure 31b and Table 4.

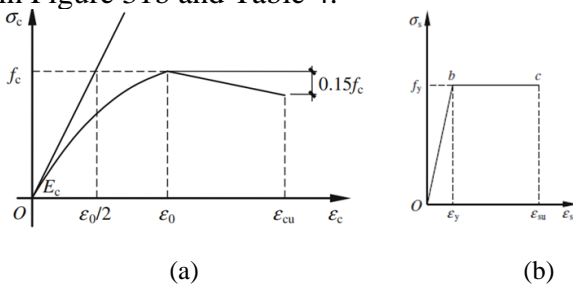


Figure 31: Concrete and reinforcement models: (a) Stress strain curve, (b) Theoretical stress–strain models of steel reinforcement (bilinear model) suggested by Hognestad [19]

$$\sigma_c = f_c' \left[ \frac{2\epsilon_c}{\epsilon_0} - \left( \frac{\epsilon_c}{\epsilon_0} \right)^2 \right] \quad (\epsilon_c \leq \epsilon_0) \quad (1)$$

$$\sigma_c = f_c' \left[ 1 - 0.15 \left( \frac{\epsilon_c - \epsilon_0}{\epsilon_{cu} - \epsilon_0} \right) \right] \quad (\epsilon_0 < \epsilon_c \leq \epsilon_{cu}) \quad (2)$$

Where:

$f_c'$ : The peak stress (the axial compressive strength of concrete).

$\epsilon_0$ : The strain corresponding to the peak stress, taking the value as  $\epsilon_0 = 2 \frac{f_c'}{E_c}$ .

$\epsilon_{cu}$ : The ultimate compressive strain, taking the value as 0.0035.

Table 3: Reinforced concrete properties

Poisson's ratio	0.2
Young's modulus (MPa)	33346
Density KN/m3	25
Uniaxial Crushing Stress ( $f_c'$ ) (MPa)	32
Uniaxial Cracking Stress ( $f_{ctr}$ ) (MPa)	3.95
Open shear Transfer Coefficient	0.3
Closed shear Transfer Coefficient	0.7

Table 4: Steel properties

Poisson's ratio	Young's modulus (MPa)	Density KN/m3	Yield stress ( $f_y$ ) (MPa)
0.3	200000	78	360

Five-cylinders models are used to do mesh sensitivity analysis using Ansys 16 [14] to choose the most appropriate mesh size. Five models with mesh sizes 0.2, 0.4, 0.6, 0.8 and 1.0 m. REINF-264 element is used to model the reinforcement as one layer within the section for vertical and horizontal reinforcement with 2.5 % reinforcement ratio as shown in the following Figure 32. Distributed load is applied on the top of the cylinder around the outer edge of the cylinder to do mesh sensitivity analysis.

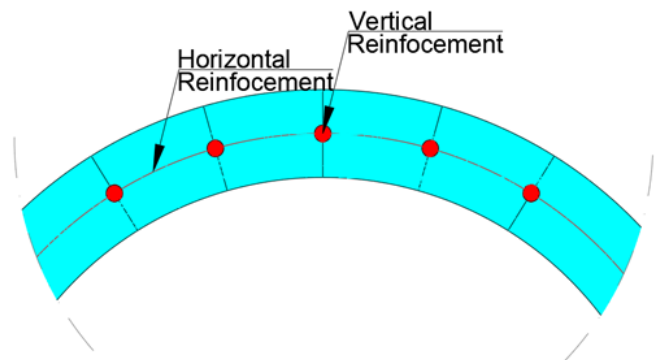


Figure 32: Reinforcement model used in Ansys16 [14]

### 5.2 MESH SENSITIVITY ANALYSIS RESULTS

From the results it is obtained that the load displacement curves are almost identical to the steel yielding point at  $f_y = 360$  MPa as shown in Figure 33. After yielding point there are differences happened especially in mesh size 1.0 m. The maximum tension happens from one side (Loads side) and the compressions happen in the opposite side. At the maximum compression of steel side, the concrete reach to nearly 22 MPa in the five mesh types which less than the compression maximum strength of concrete 35 MPa and the corresponding compression stress in the steel reaches almost 160 MPa. The results shows that the different five mesh sizes of reinforced concrete cylinders almost give the same results. The results show that the maximum stress in concrete does not reach the crushing stress as the failure type is tension failure which means the steel is yielding before crushing of the concrete. From the results the most appropriate mesh size is 0.8 m. So, for the silos with bigger diameter, the chosen mesh size will be ratio of their diameters and the tested cylinder diameter (3m), so the mesh size will be 1m for silo with diameter 7m, 2m for silo with diameter 15 m and 3m for silo with diameter 20 m.

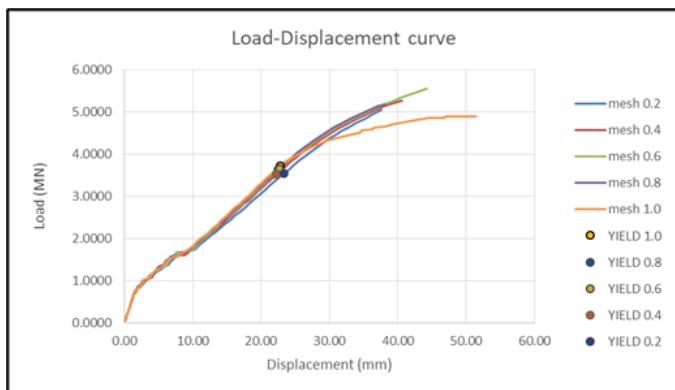


Figure 33: Load-Displacement curve for different mesh sizes.

### 5.3 PUSHOVER DATA

Various three diameters are chosen to implement Pushover Analysis (Nonlinear static analysis). Empty and full of grains silos with and without openings with diameter 7m, 15m, and 20m are chosen to establish Pushover Analysis (Nonlinear static analysis). Pushover analysis is established in two directions X and Y direction to show the difference in results especially in case of silos with opening. Different height to diameter ratio is chosen 1.5, 2.0, 2.5 and 3.0. The used reinforcement ratio to implement pushover analysis is 2.5 % for all different tested silos. The final number of models is 72 models. Applied load is a triangular load around the outer diameter of the silo as shown in the following Figure 34.

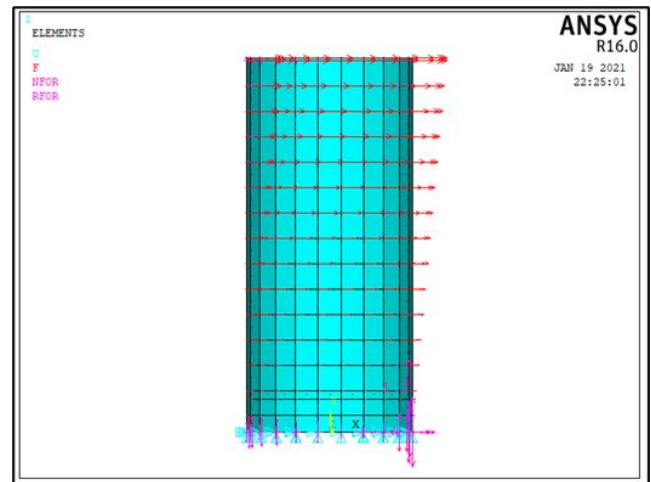


Figure 34: Applied Loads at silos to implement pushover analysis.

### 5.4 Pushover Results

The studied cases were empty and full of grains silos, with and without opening. The chosen silo diameters were 7m, 15m and 20m. Four heights to diameter ratio are established like 1.5D, 2.0D, 2.5D and 3.0 D. Load displacement curves are established to distinguish which silo cases will be more critical during earthquake effect.

Figure 35 shows load displacement curve for empty and full of grains silo without openings for diameter 20 m. It has been observed from the curve that empty silos have more displacements than full of grains silos at the yield point, as empty silos have less mass and stiffness. It also observed that the load at yield of steel point in case of empty silos is more than the yield load in case of full silos. It is obtained from the curve that the less height to diameter ratio the more resistance to lateral load as the lower of the height the more of stiffness and rigidity.

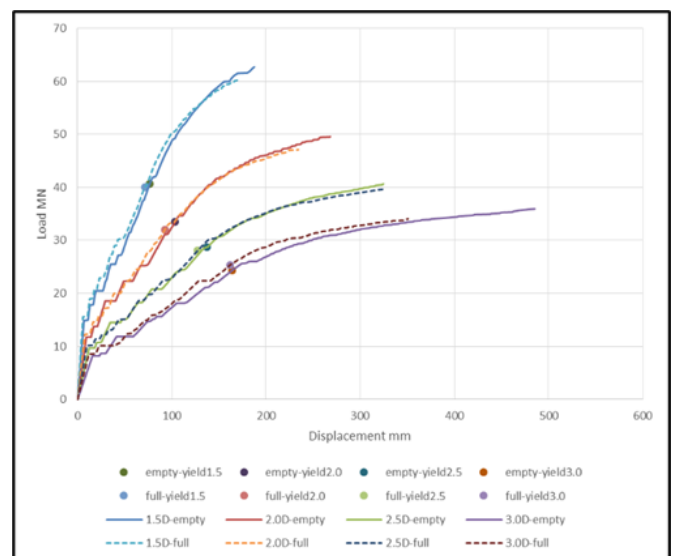


Figure 35: Load displacement curve for empty and full silo without openings for diameter 20 m.

Silos with openings are also studied by applying lateral loads in X and Y directions. Two openings with dimensions 3m width and 4 m height. Figure 36 shows load displacement curve in X direction for silo with diameter 20 m with opening for empty and full of grains silo with opening for various height to diameter ratio. It is obtained from the curve that full of grains silo has more resisting load as it is obvious at yield point as it has more stiffness due to the filling material. The less height to diameter ratio the more displacement and resisting load at yield point. In the opposite Figure 37 shows load displacement curve due to acting lateral load in Y direction for silo with diameter 20m with opening for empty and full silo with opening for various height to diameter ratio. It is obtained from the curve that full of grains silo has more load and it is obvious at yield point. The less height to diameter ratio the more displacement and load at yield point.

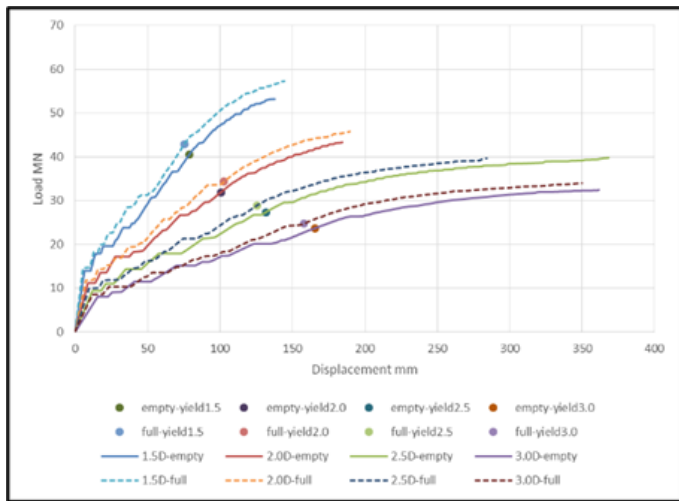


Figure 36: Load displacement curve for empty and full silo with openings for diameter 20 m for load in X direction.

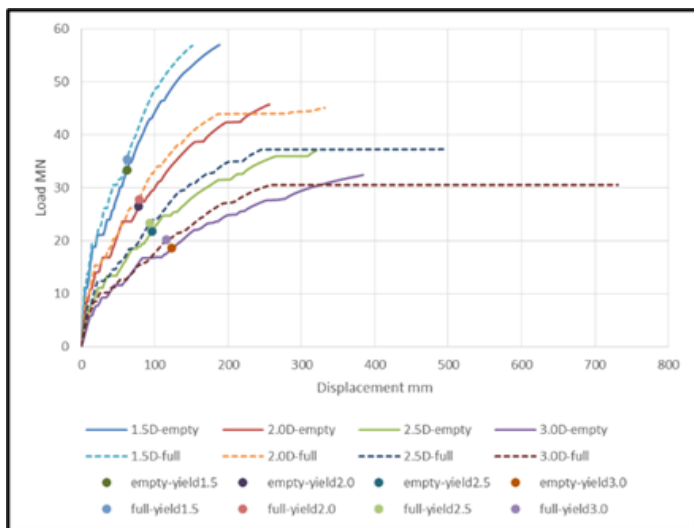


Figure 37: Load displacement curve for empty and full silo with openings for diameter 20 m for load in Y direction.

Figure 38, and Figure 39 show the difference in load resistance between loading in X and Y direction for empty silos with two opening facing each other in the bottom wall for silo diameter 20 m, and 7m respectively. It is observed from the curve that while the load being in X-direction perpendicular to the openings, the silo resists more than if the load is in Y-direction parallel to the openings., as the existing of the openings leads to decrease the stiffness of the silo in X-direction than Y-direction. Also, it is obtained that the load which makes the reinforcement yield in X-direction is more than in Y-direction.

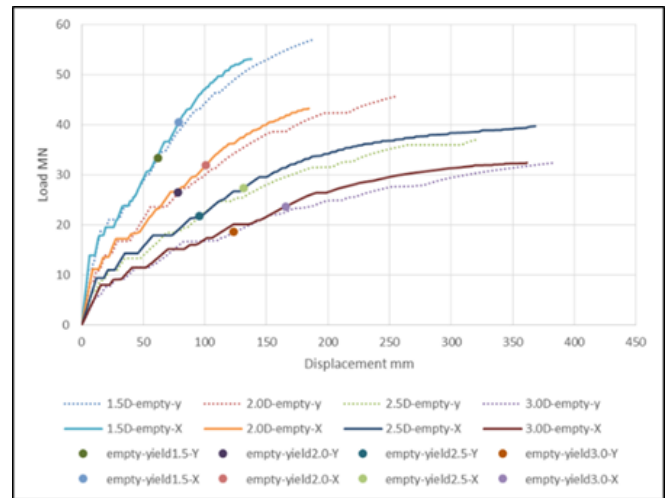


Figure 38: Load displacement curve for empty silo diameter 20 m with opening for X and Y direction.

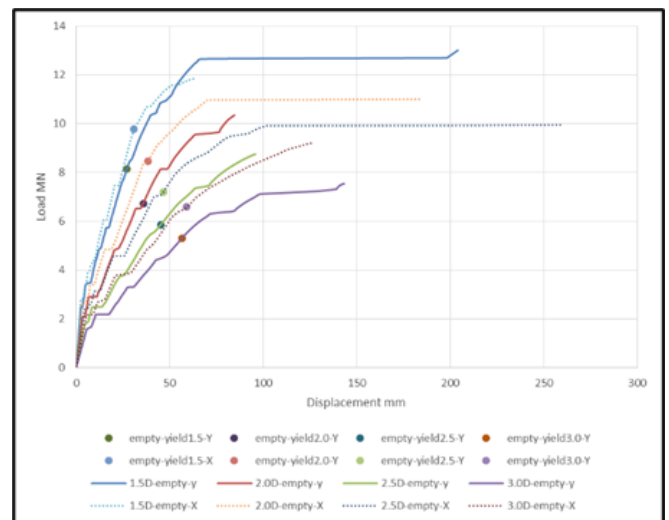


Figure 39: Load displacement curve for empty silo diameter 7 m with opening for X and Y direction.

## 6 CONCLUSION

Based on the conducted free vibration and response spectrum analyses for flat bottom clinker silos, it is observed that:

- 1- Silo's fundamental period increases with increasing height, diameter, or volume of stored material. This applies for silos with and without wall openings. Nevertheless, the effect of silo's height on its fundamental period is more pronounced than the effect of its diameter.
- 2- Existence of openings in silos' bottom walls has a significant effect on their fundamental periods; this effect decreases as the ratio of openings' length to the total wall perimeter ( $\lambda$ ) decreases, and becomes negligible for  $\lambda \leq 0.13$
- 3- The fundamental period for all studied types can be fairly estimated using the proposed formula (Eq. in clause 3.4). This formula does not include silo walls' reinforcement ratio as it is found that the fundamental period is not sensitive to the amount of wall reinforcement.
- 4- The minimum number of mode shapes required to reach a mass participating ratio of 90% (in case of full silos) is not more than 6. In the contrary, in empty silo cases this number varies from 3 (in silo with  $D=7$  m and  $H/D=2$ ) to 55 (in silo with  $D=20$  m and  $H/D=3$ ).
- 5- For silos with wall openings, the base shear demand and the seismic capacity become different in different vertical planes where their values are larger in the plane perpendicular to the opening length (on plan).
- 6- When the silo wall reinforcement ratio was increased from 0.2% to 1.0%, its lateral load capacity increased by 0.25% (full silos with  $D \geq 15$ ).
- 7- For full silos  $D = 7.0$  m, the seismic coefficient (ratio of base shear to seismic weight) decreased from 0.08 % to 0.068 % when the  $H/D$  ratio increased from 1.5 to 3.0. It is noted that- in general- the silo seismic resistance becomes less significant as the height to diameter ratio decreases when other parameters are unchanged.

## 7 REFERENCES.

- Abbas, M. (2014), Seismic Response of Clinker Silos, Faculty of Engineering, Cairo University, Msc thesis.
- Abd El-Rahim, H. (2013). Response of Cylindrical Elevated Wheat Storage Silos to Seismic Loading. *Journal Of Engineering Sciences*, 41 (6), 2079-2102.
- American Concrete Institute. (1996). Standard Practice for Design and Construction of Concrete Silos and Stacking Tubes for Storing Granular Materials.
- Ansys (2016), Ansys help viewer SAS IP, inc.
- Arar, M. (2016). Elastic Properties of Cement Phases Using Molecular Dynamic Simulation. Doctoral dissertation, Ryerson University.
- Beg, M., & Yadav, A. (2017). Seismic Analysis of Elevated Steel Silos Under Different Filling Conditions, *International Journal of Engineering and Advanced Technology (IJEAT)*, Vol. N0.5, Issue No.4.
- British Standards Institution. (2005). Eurocode 8: Design of Structures for Earthquake Resistance. London: British Standards Institution.
- Butenweg, C., Rosin, J., & Holler, S. (2017). Analysis of Cylindrical Granular Material Silos under Seismic Excitation. *Buildings*, 7(4), 61.
- Carson, J., & Craig, D. (2015). Silo Design Codes: Their Limits and Inconsistencies. *Procedia Engineering*, 102, 647-656.
- Castiglioni, C. A., Kanyilmaz, A., & John, B. (2015). Simplified Numerical Modeling of Elevated Silos for Nonlinear Dynamic Analysis. *International Journal of Earthquake Engineering*, XXXIII (1-2), CTA.
- Code, I. S. (2002). (Part 1), Criteria for Earthquake Resistant Design of Structures. Bureau of Indian Standards, New Delhi, India.
- El-Arab, I. E. (2014). Seismic Analysis of RC Silos Dynamic Discharge Phenomena. *Int. J. Eng. Adv. Technol.*, 4, 91-99.
- European Committee for Standardization. (2006) EN 1991-4: Actions on Structures-Part 4: Silos and Tanks.
- Gallego, E., Ruiz, A., & Aguado, P. (2015). Simulation of Silo Filling and Uischarge using ANSYS and Comparison with Experimental Data. *Computers and Electronics in Agriculture*, 118, 281-289.
- Gudehus, G. (1996). A Comprehensive Constitutive Equation for Granular Materials. *Soils And Foundations*, 36(1), 1-12.
- Holler, S., & Meskouris, K. (2006). Granular Material Silos under Dynamic Excitation: Numerical Simulation and Experimental Validation. *Journal of Structural Engineering*, 132 (10), 1573-1579.
- Jagtap, P., Chakraborty, T., & Matsagar, V. (2014). Nonlinear Dynamic Behavior of Granular Materials in Base Excited Silos. *Mechanics of Advanced Materials And Structures*, 22 (4), 313-323.
- Janssen, H. A. (1895). Versuche uber getreidedruck in silozellen. *Z. Ver. Dtsch. Ing.*, 39 (35), 1045-1049.
- Maj, M. (2017). Some Causes of Reinforced Concrete Silos Failure. *Procedia Engineering*, 172, 685-691.
- Nateghi, F., & Yakhchalian, M. (2011). Seismic Behavior of Reinforced Concrete Silos Considering Granular Material-Structure Interaction. *Procedia Engineering*, 14, 3050-3058.
- Niemunis, A., & Herle, I. (1997). Hypoplastic Model for Cohesionless Soils with Elastic Strain range. *Mechanics Of Cohesive-Frictional Materials*, 2 (4), 279-299.
- Pieraccini, L., Palermo, M., Stefano, S., & Trombetti, T. (2017). On the Fundamental Periods of Vibration of Flat-Bottom Ground-Supported Circular Silos contain-

- ing Gran-like Material. *Procedia Engineering*, 199, 248-253.
- Pieraccini, L., Silvestri, S., & Trombetti, T. (2015). Refinements to The Silvestri's Theory for The Evaluation of The Seismic Actions in Flat-Bottom Silos Containing Grain-Like aterial. *Bulletin of Earthquake Engineering*, 13 (11), 3493-3525.
- Rombach, G. A., & Neumann, F. (2004). 3-D Finite Element Modelling of Granular Flow in Silos. In *The 17th ASCE Engineering Mechanics Conference*.
- Silvestri, S., Gasparini, G., Trombetti, T., & Foti, D. (2012). On the valuation of the Horizontal Forces Produced by Grain-Like Material inSide Silos During Earthquakes. *Bulletin Of Earthquake Engineering*, 10 (5), 1535-1560.
- Togarsi, R. (2015). Seismic Response of Reinforced Concrete Silos. *International Journal of Research in Engineering and Technology*, 04 (09), 174-178.
- Von Wolffersdorff, P. (1996). A Hypoplastic Relation for Granular Materials with a Predefined Limit State Surface. *Mechanics of Cohesive-Frictional Materials*, 1 (3), 251-271.